© creative commons

Scientific paper

Quercetin-3 Sulfate: A Novel Inhibitor Targeting Helicobacter Pylori Revealed through Molecular Docking and Dynamic Simulations

Mohammed Baqur S. Al-Shuhaib^{1,*} , Hayder O. Hashim² , Mudher K. Mohammed³ , Jafar M. B. Al-Shuhaib⁴

¹ Department of Animal Production, College of Agriculture, Al-Qasim Green University, Al-Qasim 51013, Babil, Iraq

² Department of Clinical Laboratory Sciences, College of Pharmacy, University of Babylon, Babil 51001, Iraq.

³ Department of Pharmacy, Al-Manara College of Medical Science, Iraq

⁴ College of Medicine, University of Warith Al-Anbiyaa, Karbala, 56001, Iraq

* Corresponding author: E-mail: mohammed79@agre.uoqasim.edu.iq

Received: 05-21-2025

Abstract

Type II dehydroquinase (DHQase) is a pivotal enzyme in the synthesis of aromatic amino acids essential for *Helicobacter pylori*'s survival. It possesses distinctive characteristics and exhibits limited sequence or structural similarity to other bacterial organisms. Molecular docking was employed to screen Middle Eastern medicinal plants to identify the most promising candidates for inhibiting DHQase with the highest affinity. Docking against DHQase was performed on 2,213 ligand conformers derived from 151 natural Middle Eastern medicinal plants. Ten hits with the most favorable docking scores were selected for subsequent ADMET assay analysis and molecular dynamic simulation. Of all of the top hits, quercetin-3 sulfate had the highest docking score. This compound adhered to the druglikeness roles and demonstrated no toxicity. MD simulations indicated that the quercetin-3 sulfate-DHQase complex exhibited higher levels of stabilized RMSD and higher values of stably contributed amino acid residues than other structures. This study underscores the novel inhibitory potential of quercetin 3-sulfate against DHQase, demonstrating the highest ligand affinity. This observation suggests the validity of quercetin 3-sulfate as a potent drug for combating *H. pylori* infection.

Keywords: Eradication; Helicobacter pylori; Ligands conformers; molecular docking; natural inhibitors

1. Introduction

A major worry in the increasingly global issue of antibiotic resistance is commonly attributed to *Helicobacter pylori* infection. This bacterial infection has become a major cause behind the growing global issue of antibiotic resistance. Similar to the challenge posed by bacterial resistance to antibiotics, ^{1,2} traditional antibiotics to eliminate *H. pylori* have been hindered by the pathogen's ability to resist these treatments. Consequently, these bacteria have emerged as a severe and life-threatening disease that is challenging to manage. Furthermore, in addition to the lack of effective antibiotic therapies,³ these bacterial organisms are not new but have evolved over thousands of years and resemble many friendly bacteria found naturally

in the human body as part of its normal flora. This has made it very complex to try eliminating these pathogens that can resist many hostile host environments, which normally happens when people are ill.⁴ In terms of complex infections, this has been a new era of drug discovery through high-throughput computational methods. The recent employment of the subtractive in silico method has helped identify a few potential drugs against *H. pylori*. Many targets have recently attracted attention due to their unique roles in initiating and progressing *H. pylori* infection. These suggested targets differ from those found in non-pathogenic organisms by structure and biochemistry properties. Among these most important druggable targets is type II dehydroquinase (DHQase), also known as 3-dehydroquinate dehydratase (Enzyme Commission or

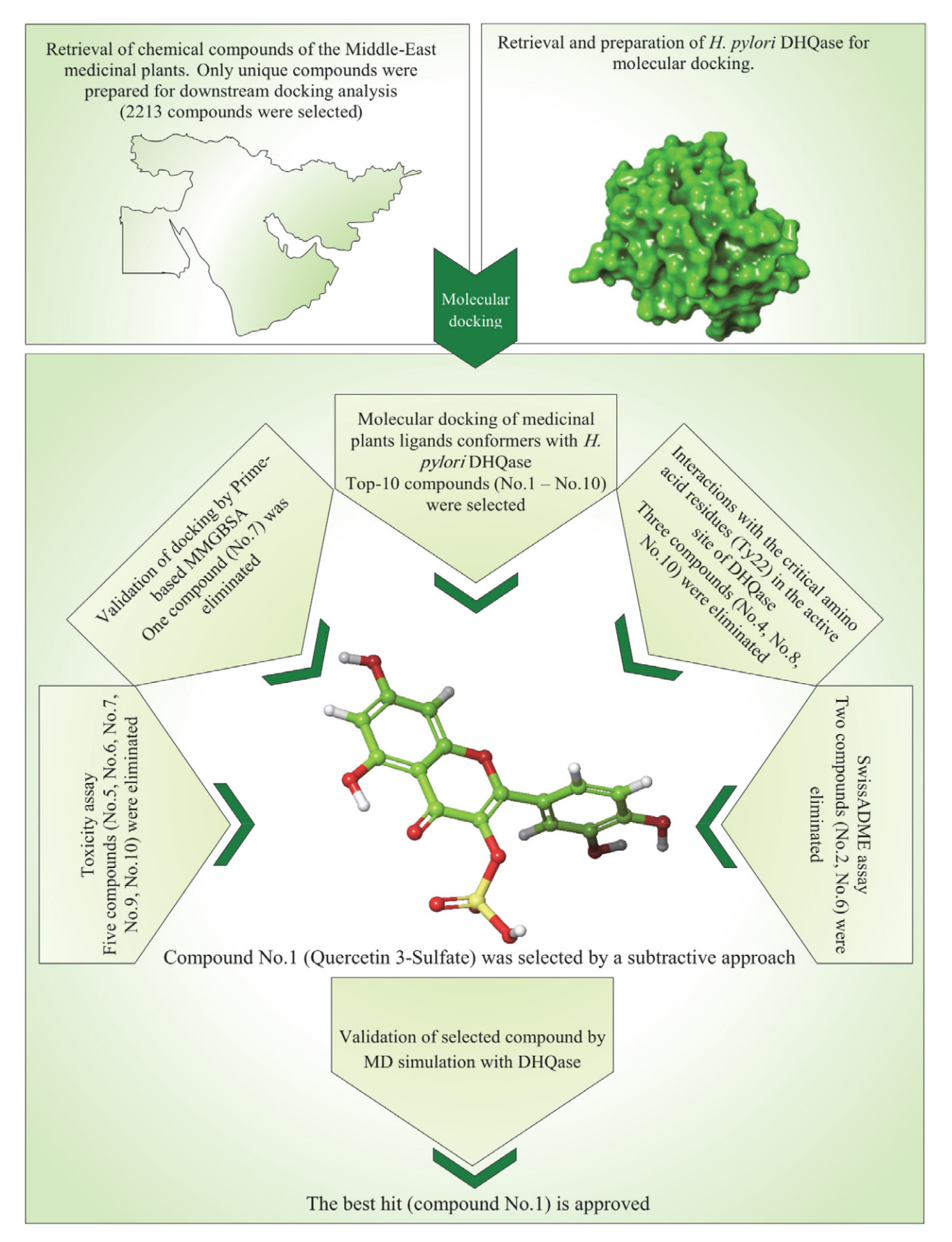


Fig. 1. Working flow of this research works from compound retrieval to molecular dynamics simulations.

EC 4.2.1.10), which emerges as a fascinating candidate for inhibition owing to its involvement in vital processes essential for the survival of H. pylori.6 This particular enzyme belongs to the lyases class and plays a critical role in the disease process initiated by H. pylori. This enzyme is distinguished by its active role in the biosynthesis of aromatic amino acids, namely tryptophan, tyrosine, and phenylalanine.7 These amino acids are essential constituents for the synthesis of proteins and are vital contributors to diverse cellular processes and signaling pathways. By partaking in the biosynthetic pathways of these aromatic amino acids, this enzyme is instrumental in shaping the adaptability and persistence of H. pylori within the gastric environment, thereby elucidating its integral role in the pathogenic mechanisms of this bacterium. It also facilitates trans-dehydration through the utilization of an enolate intermediate within the bacterial shikimate pathway. The synthesis of aromatic amino acids in bacteria is a long and complicated biochemical network that involves this biological process.8 The overall efficiency of the bacterial shikimate pathway is enhanced by DHQase, which operates through the creation and manipulation of an enolate intermediate to direct the trans-dehydration reaction. Attracting significant scientific attention as an ideal target for fighting H. pylori infections, this enzyme has been studied due to its absence in mammalian cells and retention of DHQas. Likewise, with no shikimate pathway in mammals and highly conserved sequences within DHQas, there has been considerable research interest into them as potential targets for therapeutic intervention against H. pylori. The fact that there is no shikimate pathway in mammals highlights how specifically targeting bacterial systems may be possible through DHQase and thus could be developed as therapeutics aimed at addressing H. pylori infection. The conserved sequences within DHQase further enhance its attractiveness as a target, suggesting a fundamental and crucial role in bacterial physiology that could be strategically exploited for therapeutic purposes. Consequently, DHQase represents a significant target for eradicating these highly dangerous pathogens. Hence, a range of approaches can be employed to formulate potent drugs targeting DHQase with the aim of impeding its functionality within the bacterial shikimate pathway. One of the most pressing strategies that should be explored for the suppression of DHQase activity involves the employment of molecular docking and molecular dynamic (MD) simulation approaches.^{9,10} These methodologies provide a precise screening tool for identifying the most effective drug to efficiently inhibit DHQase, minimizing the need for excessive time, financial resources, or labor. Given the numerous constraints associated with budgetary limitations and time-consuming traditional wet lab experiments, computational tools have become increasingly essential for rapidly pinpointing the most effective inhibitors for complex diseases.¹¹ Consequently, molecular docking has demonstrated remarkable outputs within a considerably shorter

timeframe when compared to classical experiments, which may necessitate prolonged experimental validation before being considered for potential human use. Conversely, plant extracts have long been prescribed in many Middle Eastern regions for alleviating various gastrointestinal symptoms. However, the active chemical compounds within these medicinal plants have yet to be explored for their potential to combat *H. pylori* infection using cutting-edge *in silico* tools. Therefore, the virtual screening of these natural resources presents an intriguing opportunity to discover the most potent compound capable of deactivating *H. pylori* DHQase, which may not have been identified in other parts of the world.

To the best of our knowledge, no naturally occurring inhibitor has been developed to demonstrate notable effectiveness in inhibiting *H. pylori* DHQase while simultaneously possessing a favorable drug-like profile. In this study, a total of 2,213 ligand conformers were prepared from 151 medicinal plants commonly found in various regions of the Middle East and subjected to docking against DHQase. The goal was to identify the most potent compound for deactivating this enzyme, considering both favorable drug-like properties and dynamic characteristics. The entire workflow of our study is illustrated in Fig. 1.

2. Materials and Methods

2. 1. Molecular Docking Setup

The Schrodinger suite, notably Maestro Version (12.8).117 in conjunction with MMshare Version (5.4.117), Release 2021-2, operating on the Windows-x64 platform, was utilized for all molecular docking investigations. This robust suite enabled a spectrum of critical functions, encompassing ligand preparation, protein structure refinement, molecular geometry minimization, and binding affinity predictions in ligand-protein interactions. Moreover, Maestro's intuitive graphical interface was employed to generate detailed three-dimensional (3D) visualizations, illustrating the interactions and bonds established between key amino acid residues and the primary ligands involved.

2. 2. Ligand Selection and Preparation

A diverse array of natural compounds was derived from an extensive compilation of 151 medicinal plants chronicled in Dr. Duke's phytochemical and ethnobotanical database. The United States Department of Agriculture (USDA) (http://phytochem.nal.usda.gov) has compiled this invaluable resource, which contains extensive information on phytochemicals and their biological activities.

The natural compounds investigated represent an expansion of our previously published dataset, which has been purposefully broadened to include medicinal plants endemic to the Middle East. ^{12–14} This curated collection was specifically employed as the ligand pool for subse-

quent molecular docking studies targeting the enzyme DHQase. To facilitate the docking process, structural data file (SDF) representations of these ligands were sourced from the PubChem web server.¹⁵ In preparation for molecular docking, we diligently removed redundant structures from the selected natural compounds, yielding a refined set of unique ligands ready for further analysis. These ligands underwent a rigorous optimization process via the Ligprep module, a crucial component of the GLIDE software suite. Notably, ligands containing more than 500 atoms were systematically excluded in adherence to the default parameters established by Ligprep. Following optimization, we calculated the partial atomic charges of the refined ligands, employing the default settings of the OPLS4 force field. The resulting optimized ligands were subsequently utilized in the molecular docking experiments with DHQase, paving the way for insights into potential therapeutic applications.

2. 3. Protein Preparation

The H. pylori dehydroquinate synthase (DHQase), particularly the variant represented by chain A, is cataloged in the UniProtKB database under accession number Q(48255), with additional details accessible at the UniProt website (https://www.uniprot.org/). This enzyme, encoded by the aroQ gene, consists of a total of 157 amino acids, underscoring its relatively small yet functionally significant structure. The three-dimensional crystallized structure of H. pylori DHQase has been extensively documented and can be retrieved from the Protein Data Bank server using the identifier PDB ID 4B6R. The model obtained represents the holoenzyme form of DHQase, consisting of three identical polypeptide chains, each containing 157 amino acids, with an impressive resolution of (2.00) Å, which attests to the quality of the crystallographic data. Upon isolating chain A from this structure, we focused on identifying the active site, vital for mediating direct interactions with the substrate in the shikimate pathway-a fundamental metabolic route in many bacteria and plants. To prepare the retrieved DHQase structure for further analysis, we employed the protein preparation wizard tool available within the Maestro software suite. This preparation optimized the molecular conformation by accurately arranging the bonds and incorporating necessary hydrogen atoms into the structure. Subsequently, an energy minimization protocol was executed at a neutral pH of (7.0), utilizing the default settings of the OPLS4 force field to ensure stability. To ensure precision during this optimization, a stringent cut-off Root Mean Square Deviation (RMSD) value of (0.30) Å was implemented, enabling us to achieve a high degree of accuracy in the refined structure of the enzyme. Within the active site of DHQase, it has been reported that two amino acid residues (Tyr22 and His102) played a pivotal role in the enzyme activity in mediating interactions with the substrate.16 Tyr22 is essential in enhancing DHQase binding affinity by engaging in numerous interactions with aromatic functional groups of substrates and inhibitors. ¹⁷ While Tyr22 acting as the base in the enzymatic mechanism, His102 is involved in the final step of substrate conversion. This action is attributed to the involvement of His102 in forming hydrogen bonds with the substrate, contributing to the overall stability of the enzyme-substrate complex. Furthermore, His102 plays a key role in the binding of various inhibitors, indicating its importance in the active site dynamics.⁷ Due to the essential roles reported in the DHQase activity, both residues were selected as the centers of the receptor grid during the grid generation process. Accordingly, the receptor grid was centered at the Cartesian coordinates (x = 26.315, y =50.926, z = -12.143), with an outer grid box of $30 \times 30 \times 30$ Å and an inner (ligand) grid box of $10 \times 10 \times 10$ Å.

2. 4. Molecular Docking Procedure

A receptor grid was prepared with adjusted van der Waals radii (1.0) Å, and a charge cutoff polarity score of (0.25) Å was applied to refine the interactions. A comprehensive selection of 2,213 ligand conformers was systematically optimized and subsequently subjected to a docking procedure against the receptor grid designed explicitly for DHQase. This process was conducted under the OPLS4 force field, which provided a robust framework for accurately simulating the interactions between the prepared ligands and the enzyme. The docking utilized the Standard Precision (SP) tool, thoroughly exploring potential binding configurations. Following the docking procedure, the top ten ligand-protein complexes exhibiting the highest SP docking scores were meticulously selected for further investigation. To deepen our understanding of these promising candidates, additional chemical properties were assessed using the ClassyFire tool, which categorizes compounds based on their structural and functional attributes. This multi-faceted approach highlights the significance of Tyr22 and His102 in substrate interaction and underscores the meticulous methods employed in identifying potential natural inhibitors of DHQase.

2. 5. Binding Free Energy Calculations

A comprehensive evaluation of the binding free energies associated with the docked structures was conducted to assess the efficacy of the docking process. This assessment utilized Prime-based MMGBSA (Molecular Mechanics – Generalized Born Surface Area) calculations, 18 which are recognized for their sophistication in analyzing molecular interactions. Specifically, the analysis involved positioning the top ten compounds within a solution formulated using the default Optimized Potential for Liquid Simulations (S-OPLS) force field, a Schrödinger software suite standard feature. The binding free energy $(\Delta G_{\rm bin})$ for the most promising compounds was calculated

through a detailed equation, emphasizing the importance of precise numerical analysis in understanding the stability and interaction strengths of the docked complexes. The equation $\Delta G_{\rm bin} = \Delta E_{\rm mm} + \Delta G_{\rm sol} + \Delta G_{\rm SA}$ provides a comprehensive framework for grasping the binding energy between a receptor and a ligand. In this regard, $\Delta E_{\rm mm}$ denotes the difference in minimized energy (mm) between the two entities. This parameter reflects the inherent energy of both the receptor and the ligand in their unbound, or 'free,' states. Essentially, $\Delta E_{\rm mm}$ captures the energetic relationship that emerges when the receptor and ligand approach one another, elucidating how their respective energies influence binding.

Additionally, ΔG_{sol} represents the change in solvation energy (sol) that transpires as the receptor and ligand interact. This term also accounts for the energies of both the free receptor and the free ligands, 19 emphasizing the role of the surrounding solvent in modulating their interaction. The solvation energy can significantly influence how these molecules behave in a biological context, as it reflects solvation's energetic cost or benefit when the molecules come into proximity. Conversely, ΔG_{SA} indicates the variation in surface energy (SA) that occurs during the interaction between the receptor and the ligand.²⁰ Like the other terms, this variation also considers the free receptor's and free ligands' energies. Surface energy is pivotal as it pertains to how the molecules orient and adhere to each other, which can be affected by molecular shape and functional groups. This equation encapsulates the intricate interplay of minimized energy differences, solvation effects, and surface energy considerations that collectively determine the binding affinity between a receptor and a ligand. While each term is integral to understanding the energetic landscape of molecular interactions between ligand and receptor, the entropic contribution $(-T\Delta S)$ was not included in the present calculations. The entropic contribution that is typically included in full binding free energy calculations has been omitted in this study. This is consistent with standard MMGBSA protocols due to the high computational cost and complexity related to the robust estimation of entropy. Furthermore, because our primary focus was on relative binding affinities among compounds, the entropic term is expected to have a lesser impact on the relative ranking of ligands.

2. 6. ADME and Toxicity Predictions

We undertook an exhaustive evaluation of the ten ligands that achieved the highest SP docking scores, with the primary aim of exploring their Adsorption, Distribution, Metabolism, and Elimination (ADME) properties. This detailed analysis was performed utilizing the SwissADME web server.²¹ By submitting the SMILES structures of these compounds to the server, we assessed various aspects of their pharmacokinetics, drug-likeness, and bioavailability. To further enrich our understanding of

these ligands, we also employed the Protox-II server as a virtual laboratory to predict potential risks associated with hepatotoxicity, carcinogenicity, immunogenicity, mutagenicity, and cytotoxicity for the same small molecules.²² Compounds identified as potentially toxic were systematically excluded from subsequent analyses to ensure safety and efficacy in our findings.

2. 7. Molecular Dynamics Simulations

We employed Desmond version 2020, utilizing the OPLS3e force field for the molecular dynamics simulation study to enhance accuracy and reliability. In the preliminary phase, we meticulously cleaned and optimized the docked complexes to achieve an ideal arrangement of hydrogen bond networks. The TIP3P water model was adopted to effectively simulate solvation effects, while periodic boundary conditions were integrated to establish a realistic molecular dynamics (MD) environment. To ensure charge neutrality and physiological ionic strength, 18 sodium (Na⁺) and 18 chloride (Cl⁻) ions (corresponding to 0.15 M NaCl) were added to each system. After ion addition, the control-1 (DHQase-avicularin) complex contained 21,808 atoms, the control-2 (DHQase-galangin) complex contained 21,831 atoms, and the best candidate (DHQase-quercetin 3-sulfate) complex contained 21,819 atoms.²³ Energy minimization of each system was performed in Schrödinger Desmond using its default hybrid steepest-descent/LBFGS algorithm. A multi-stage heating protocol was applied between minimization and NPT equilibration: initial Brownian-dynamics NVT at 10 K, followed by standard NVT equilibration, and finally transition to NPT production conditions at 300 K. Subsequent NPT simulations employed the Martyna-Tobias-Klein barostat with a relaxation time of 2 picoseconds and isotropic pressure coupling at 1.01325 bar.²⁴ To address distance constraints for small molecules during the MD simulations, we implemented the SHAKE algorithm, ensuring that the geometry, bond angles, and bond lengths of heavy atoms were appropriately maintained in the presence of water molecules. Throughout the simulation, we preserved a continuous system with long-range electrostatics, employing the particle mesh Ewald method to maintain periodic boundary conditions. The NPT ensemble was utilized to equilibrate the system, effectively maintaining a pressure of (1.01325) bar and temperature of 300 K for a duration of 100 nanoseconds.²⁵ Following these dynamic simulations, we conducted a thorough analysis of the resultant trajectories to compute variable criteria, including Root Mean Square Deviation (RMSD) and Root Mean Square Fluctuation (RMSF) for the complex formed between DH-Qase and the most promising ligands. This rigorous analysis was designed to assess the stability of the docked complexes under the dynamic conditions of the simulation, providing critical insights into their behavior and interactions.

3. Results

To identify the lead compound with the most promising properties for inhibiting DHQase, we used an array of molecular docking, Prime-MMGBSA analysis, ADMET evaluation, pharmacokinetic toxicity prediction, and MD simulation in this investigation. We harnessed the rapid advancements in cutting-edge prediction tools to screen the active compounds found in medicinal plants from the Middle East, unveiling their potential for use against DHQase.

3. 1. Molecular Docking

A total of 2,213 ligand conformers were meticulously prepared through the utilization of the ligprep module. From this extensive pool, the ten most exemplary ligands, distinguished by their superior SP docking scores against DHQase, were judiciously selected for further scrutiny.

The docking scores for these elite ligands exhibited a discernible range, spanning from -8.178 kcal/mol (encountered in quercetin 3-sulfate, identified by PubChem ID 5280362) to -7.836 kcal/mol (evident in moracin M, identified by PubChem ID 185848). Ligands possessing docking scores below this threshold were deliberately excluded from subsequent analyses, as elucidated in Table 1.

In addition to docking scores, the GLIDE tool provided a parallel validation through Glide Ligand Efficiency (GLE) values. A higher GLE score indicates a greater potential for the ligand to be bound to the receptor. Accordingly, these compounds exhibited varying GLE values, ranging from -0.435 (the highest GLE value) in moracin M to -0.18 (the lowest GLE value) in delphinidin 3-diglucoside. Within this range, quercetin 3-sulfate also demonstrated a high GLE value of -0.315. However, further evaluations were carried out to assess the affinity of these natural ligands in terms of their binding to the target enzyme, providing an additional layer of confirmation for these ligand-receptor interactions (Table 2).

It is important to note that both docking scores and GLE values alone were insufficient for assessing ligand-receptor interactions without considering the potential involvement of specific active site residues. Although a high docking score represents a theoretical prediction of binding energy, this numerical value does not provide insight into the specific molecular forces at play. This can be explained with the possibility of the obtained high docking score being generated from a ligand forming multiple weak and non-specific interactions with the receptor's surface. Furthermore, the high docking score may be generated from a single and strong interaction in a non-physiologically relevant pocket. Conversely, a less favorable docking score might correspond to a biologically significant interaction where the ligand forms crucial hydrogen bonds or salt bridges with a few key active site residues essential for the receptor's function. Although these particular interactions may have a lesser contribution to the overall numerical result, they tend to be the main cause of biological activity. For this reason, our analysis of the visual inspection of the docking poses and the identification of specific interactions with key amino acids have been combined with the docking scores to enable a more biologically meaningful interpretation of the docking results.

Among the amino acid residues located within the active site of DHQase, quercetin 3-sulfate was found to form the highest number of interactions compared to the other ligands, as depicted in Fig. 2.

The augmented quantity of interactions observed can be ascribed to the integral role played by quercetin 3-sulfate, which engendered the establishment of ten bonds with eight distinct amino acid residues situated both within and in proximity to the active site of DHQase. To elaborate this interaction, quercetin 3-sulfate fostered a singular hydrogen bond with Met13, Asp18, Asn76, Gly78, and His82, while concurrently forming dual hydrogen bonds with Arg113, in addition to a Pi-cation interaction with Arg109. Most notably, quercetin 3-sulfate exhibited strong interactions, including hydrogen bonding and Pi-Pi stacking, with the active site residue Tyr22. In contrast, aromadendrin, tricin, and moracin M did not interact with this residue, indicating a less significant inhibitory role against DHQase and potentially limiting their efficacy as potent agents against H. pylori DHQase (Fig. 3).

Table 1. The top ten Middle Eastern medicinal herbs' docking	ng scores against type II dehydroquinase of Helicobacter pylori.

No.	Title	Name	PubChem molecular formula	PubChem molecular weight (g/mol)	Docking score	Glide ligand efficiency
1.	5280362	Quercetin 3-Sulfate	C ₁₅ H ₁₀ O ₁₀ S	382.3	-8.178	-0.315
2.	5490064	Avicularin	$C_{20}H_{18}O_{11}$	434.3	-8.167	-0.263
3.	5281616	Galangin	$C_{15}H_{10}O_5$	270.24	-7.981	-0.399
4.	122850	Aromadendrin	$C_{15}H_{12}O_6$	288.25	-7.979	-0.380
5.	471	Dihydroquercetin	$C_{15}H_{12}O_7$	304.25	-7.975	-0.363
6.	5316496	Delphinidin 3-Diglucoside	$C_{27}H_{31}O_{17}^{+}$	627.5	-7.939	-0.180
7.	44123491	Isorhamnetin 3-Sulfate	$C_{16}H_{10}O_{10}S^{-2}$	394.3	-7.931	-0.378
8.	5281702	Tricin	$C_{17}H_{14}O_7$	330.29	-7.846	-0.327
9.	5487766	Persicarin	$C_{16}H_{12}O_{10}S$	396.3	-7.845	-0.291
10.	185848	Moracin M	$C_{14}H_{10}O_4$	242.23	-7.836	-0.435

Table 2. The most significant amino acid residues that interact with the targeted active site of Helicobacter pylori type II dehydroquinase in the Middle Eastern medicinal plants.

No.	Title	Name	The most important interacting amino acid residues	Total bonds
1.	5280362	Quercetin 3-Sulfate	Met13 (H-bond 1.97Å) Asp18 (H-bond 2.7Å) Tyr22 (H-bond 1.95Å and Pi-Pi stacking 4.21Å) Asn76 (H-bond 1.92Å) Gly78 (H-bond 2.72Å) His82 (H-bond 2.51 Å) Arg109 (Pi-cation 6.1Å) Arg113 (H-bond 1.99Å and H-bond 2.19Å)	10
2.	5490064	Avicularin	Met13 (H-bond 2.13Å) Arg17 (H-bond 2.79Å) Asp18 (H-bond 2.0Å) Asn76 (H-bond 1.94Å) His82 (H-bond 2.59Å) Arg109 (Pi-cation 6.04Å and Pi-cation 6.57Å) Arg113 (H-bond 2.23Å)	8
3.	5281616	Galangin	Tyr22 (Pi-Pi stacking 4.00Å) Asn76 (H-bond 1.59) Gly78 (H-bond 2.79Å) His82 (H-bond 2.60 Å) Arg113 (H-bond 2.30Å)	5
4.	122850	Aromadendrin	Arg17 (H-bond 2.36Å) Asn76 (H-bond 1.83 Å) Gly78 (H-bond 2.70Å) His82 (H-bond 2.55 Å) Arg113 (H-bond 2.20Å)	5
5.	471	Dihydroquercetin	Pro9 (H-bond 2.02Å) Tyr22 (Pi-Pi stacking 3.93Å) His82 (H-bond 1.90 Å) Arg109 (Pi-cation 5.95Å) Arg113 (H-bond 2.52Å)	5
6.	5316496	Delphinidin 3-Diglucoside	Pro9 (H-bond 2.77Å) Asn10 (H-bond 1.76Å) Arg17 (H-bond 1.62Å) Tyr22 (H-bond 2.25Å and Pi-Pi stacking 3.25Å) Hip102 (H-bond 2.08Å) Arg109 (H-bond 2.59Å)	7
7.	44123491	Isorhamnetin 3-Sulfate	Tyr22 (H-bond 2.07Å) Asn76 (H-bond 1.90 Å) Gly78 (H-bond 2.65Å) His82 (H-bond 2.52Å) Arg109 (Pi-cation 5.96Å and Salt-bridge 3.81Å) Arg113 (H-bond 2.09Å, H-bond 2.38Å, and Salt-bridge 3.59Å)	9
8.	5281702	Tricin	Met13 (H-bond 2.25Å) Asn76 (H-bond 1.90Å) His82 (H-bond 2.42Å) Arg113 (H-bond 2.08Å)	4
9.	5487766	Persicarin	Met13 (H-bond 1.97Å) Tyr22 (Pi-Pi stacking 4.25Å and H-bond 2.00Å Asn76 (H-bond 1.90Å) Gly78 (H-bond 1.92Å) His82 (H-bond 2.45Å) Arg109 (Pi-cation 6.04Å) Arg113 (H-bond 2.09Å and H-bond 2.38Å)	9
10.	185848	Moracin M	Arg17 (H-bond 2.08Å) Asn76 (H-bond 2.03Å)	2

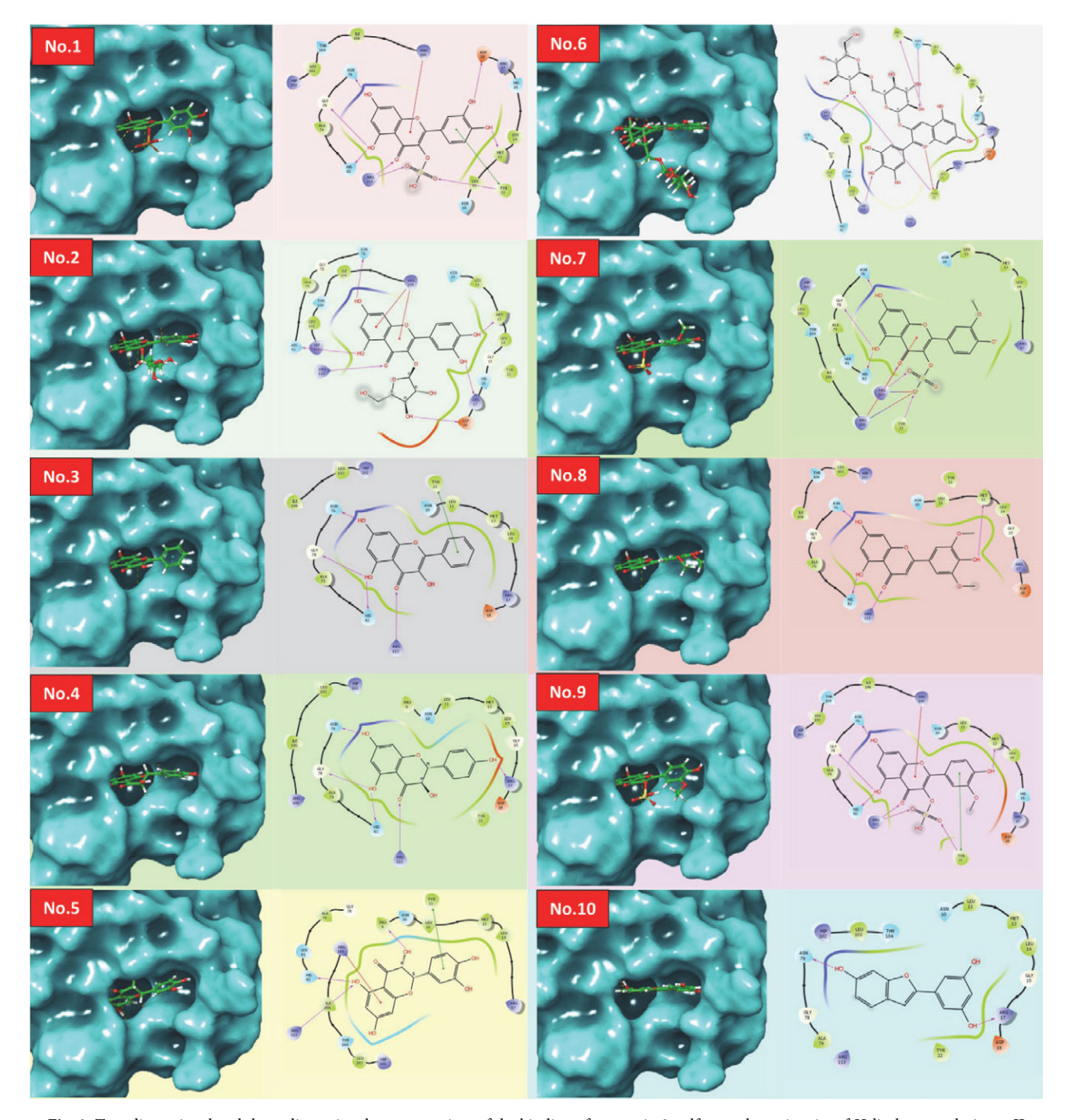


Fig. 2. Two-dimensional and three-dimensional representatives of the binding of quercetin 3-sulfate to the active site of *Helicobacter pylori* type II dehydroquinase.

3. 2. Binding Free Energy Analysis

Further validation of the observed affinity in the receptor-ligand binding interactions was performed using Prime-based MMGBSA. This tool revealed varying strengths of binding energies in the assessed receptor-ligand interactions (Table 3).

Delphinidin 3-diglucoside (PubChem compound 5316496) exhibited the highest score of MMGBSA-dG

binding energy with the targeted DHQase receptor, recording -61.62 kcal/mol, while isorhamnetin 3-sulfate (PubChem compound 44123491) displayed the lowest MMGBSA-dG binding energy at -28.02 kcal/mol. The exceptionally low MMGBSA value for isorhamnetin 3-sulfate necessitated its exclusion from further consideration. Prime MMGBSA calculations revealed that quercetin 3-sulfate possessed an MMGBSA value of -58.31 kcal/

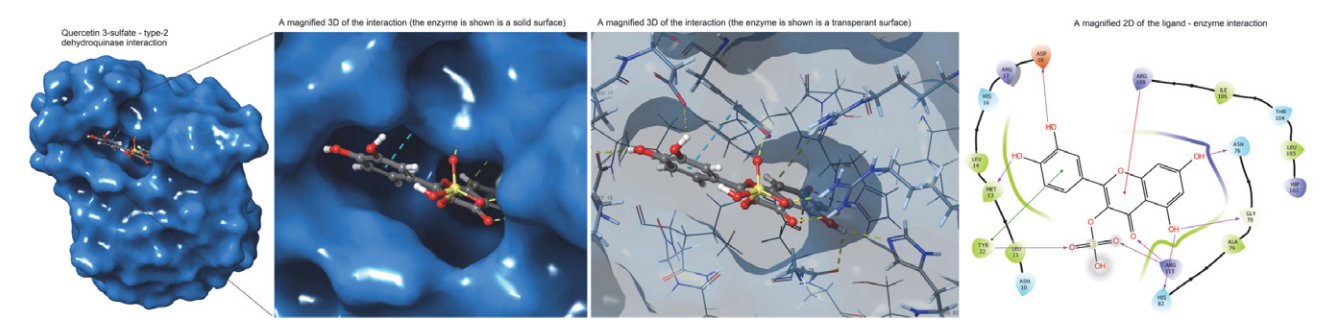


Fig. 3. The best posture contacts for the top-ranked ligands over H. pylori type II dehydroquinase. The docking score is used to align natural ligands; compound no. 1 has the highest binding affinity, while compound no. 9 has the lowest. Compound no. 10 is the control compound, which is an inhibitor of type II dehydroquinase.

Table 3. The top ten Middle Eastern medicinal plants' ligand-receptor Prime-based binding energies (MMGBSA) against Helicobacter pylori type II dehydroquinase.

No.	PubChem No.	Names	MMGBSA-dG binding energy (kcal/mol)	MMGBSA-dG bind in coulomb	MMGBSA-dG bind in covalent	MMGBSA dG bind solv GB	MMGBSA dG bind vdW
1.	5280362	Quercetin 3-Sulfate	-58.31	-47.52	4.45	41.53	-38.39
2.	5490064	Avicularin	-61.47	-49.38	8.65	37.33	-37.18
3.	5281616	Galangin	-51.23	-30.90	4.05	30.16	-36.43
4.	122850	Aromadendrin	-51.53	-33.43	9.35	29.68	-36.43
5.	471	Dihydroquercetin	-58.56	-29.75	4.74	23.13	-34.54
6.	5316496	Delphinidin 3-Diglucosid	le -61.62	10.75	4.86	-19.36	-37.09
7.	44123491	Isorhamnetin 3-Sulfate	-28.02	-67.07	5.96	91.25	-42.36
8.	5281702	Tricin	-54.19	-33.62	6.51	29.70	-38.14
9.	5487766	Persicarin	-59.67	-39.67	1.05	39.77	-41.59
10.	185848	Moracin M	-43.88	-18.41	4.97	19.62	-32.26

mol, representing a high-energy score following delphinidin 3-diglucoside, avicularin, persicarin, and dihydroquercetin, respectively. According to the MMGBSA values, the key contributors favoring the binding of these compounds to their respective receptors were attributed to MMGBSA-dG bind in Coulomb score, while MMGB-SA-dG bind vdW score was found to exhibit a secondary role in these interactions. In contrast, the score of both MMGBSA-dG bind in Covalent and MMGBSA-dG bind solv GB exhibited less favorable contributors to these binding interactions. However, the significantly low MMGBSA value of isorhamnetin 3-sulfate (–28.02 kcal/mol) limited its potential utility in inhibiting the targeted site within DHQase.

3. 3. Druglikeness Prediction

According to the SwissADME tool, quercetin 3-sulfate demonstrated some of the most favorable characteristics compared to the other top-ten ligands. To assess the appropriateness of each candidate, drug-likeness filters were applied by employing Lipinski's rule of five, providing a basis for their categorization. Quercetin 3-sulfate complied with all five of Lipinski's drug-likeness criteria,

while certain other compounds exhibited varying violations of these rules (Table 4).

Avicularin and delphinidin 3-diglucoside, for instance, displayed two and three rule violations, respectively, which diminished their potential for the intended inhibition. Furthermore, quercetin 3-sulfate exhibited low gastrointestinal (GI) absorption properties, which may enhance its effectiveness by allowing it to exert its effects locally for an extended duration within the GI tract.²⁷ Based on these data, our computations suggest that quercetin 3-sulfate possessed the highest SP docking score and strong Prime-MMGBSA scores against DHQase. Additionally, it displayed a highly specific interaction with the active amino acid residue Tyr22 and favorable drug-likeness properties. Based on these findings, quercetin 3-sulfate was the sole compound selected for further downstream predictions to assess its inhibitory dynamics on DHQase using thermodynamic parameters.

3. 4. Dynamic Simulation of Quercetin 3-sulfate with DHQase

Three distinct simulations were executed, each involving DHQase in complexation with quercetin 3-sulfate,

Table 4. The top ten compounds from Middle Eastern medicinal plants that have been shown to inhibit Helicobacter pylori type II dehydroquinase in terms of druglikeness.

No. a 1. 5280362 Quercetin 3-Sulfate 2. 5490064 Avicularin 3. 5281616 Galangin 4. 122850 Aromadendrin 5. 471 Dihydroquercetin 6. 5316496 Delphinidin 3-Diglucoside 7. 44123491 Isorhamnetin 3-Sulfate 8. 5281702 Tricin	GI absorption		Druglikeness	keness				Toxicity	
	•	BBB permeant	Lipinski rules of five	Bioavai- ability score	Hepatoxi-city city	Carcinog- enicity	Immunog- enicity	Mutagenic- ity	Cytotoxic- ity
, , , , , , , , , , , , , , , , , , , ,	ulfate Low	oN	0 violation	0.11	Inactive	Inactive	Inactive	Inactive	Inactive
• 1 :	High	No	2 violations	0.17	Inactive	Inactive	Inactive	Inactive	Inactive
, – – – ,	High	No	0 violation	0.55	Inactive	Inactive	Inactive	Inactive	Inactive
	I	No	0 violation	0.55	Inactive	Inactive	Inactive	Inactive	Inactive
	etin High	No	0 violation	0.55	Inactive	Active	Inactive	Active	Inactive
 44123491 Isorhamnetin 3 5281702 Tricin 		No	3 violations	0.17	Inactive	Inactive	Active	Inactive	Inactive
	3-Sulfate Low	No	0 violation	0.11	Inactive	Inactive	Active	Inactive	Inactive
	High	No	0 violation	0.55	Inactive	Inactive	Inactive	Inactive	Inactive
9. 5487766 Persicarin	Low	No	0 violation	0.11	Inactive	Inactive	Active	Inactive	Inactive
10. 185848 Moracin M	High	oN	0 violation	0.55	Inactive	Active	Inactive	Inactive	Inactive

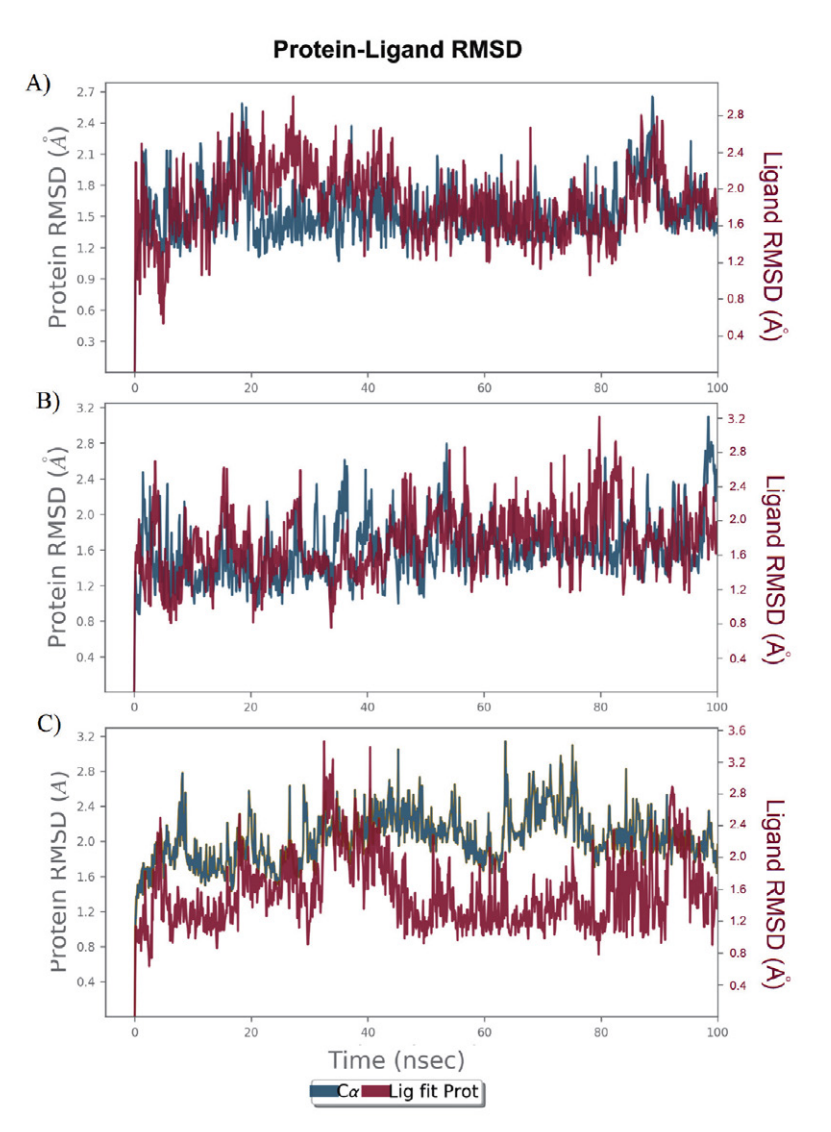


Fig. 4. Comparative RMSD simulation of *Helicobacter pylori* type II dehydroquinase complexed with quercetin 3-sulfate (in branch A), avicularin (in branch B), and galangin (branch C). MD simulations are plotted in 100 ns simulation time.

avicularin, and galangin, with the primary objective of appraising the structural robustness of DHQase in response to the interaction with these specific ligands. To delineate the flexibility inherent in the docked complexes, a meticulous examination of the RMSD from the simulated trajectories was undertaken. Notably, the DHQase complex with quercetin 3-sulfate demonstrated an average RMSD maintaining a level below 2 Å, achieving a state of dynamic equilibrium in a brief timeframe of less than 5 ns. This observation suggests a strong affinity between quercetin 3-sulfate and the DHQase target, forming a stable complex. Notably, the MD simulation revealed that the conformational changes in the complex did not pose significant challenges, further indicating their effective binding (Fig. 4a).

Similarly, the mean RMSD of the DHQase in conjunction with the avicularin compound was likewise confined to a value below 2 Å, and the concomitant complex swiftly attained a state of dynamic equilibrium. This underscores the efficacy with which avicularin selectively targets DHQase, engendering the formation of a robust and stable complex

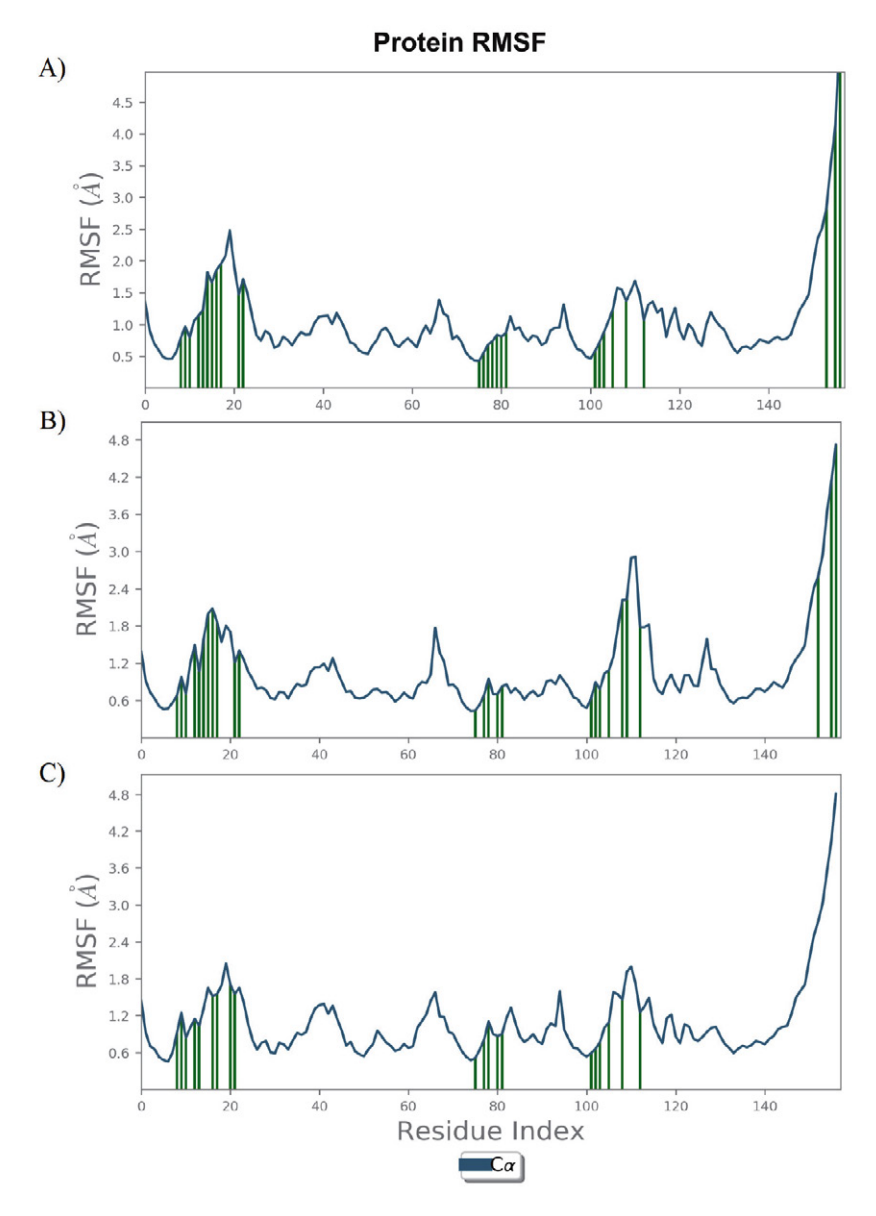


Fig. 5. Comparative RMSF simulation of *Helicobacter pylori* type II dehydroquinase complexed with quercetin 3-sulfate (in branch A), avicularin (in branch B), and galangin (branch C).

(Fig. 4b). Comparing these two complexes; it is evident that both exhibit good stability, remaining securely within the active pocket of DHQase. This underscores the high binding efficiency and inhibitory characteristics of both compounds. Conversely, the average RMSD of the DHQase with the galangin compound exceeds 2 Å, indicating a less stable complex. This implies that the diminutive galangin molecule encounters challenges in establishing a steadfast confluence with the designated protein, as illustrated in Fig. 4c. Moreover, the discernible lack of constancy exhibited by galangin, as it disengages from the active pocket of DHQase, serves as an indicative manifestation of diminished binding efficiency and inhibitory attributes for this particular compound.

By inspecting ligand's contacts with the DHQase amino acid residues in the RMSF plot, it has been shown that quercetin 3-sulfate exhibited 27 contacts with residues located at several key positions within DHQase. Since various contacts with DHQase amino acids showed more reduced RMSF values, a more stable engagement of quercetin 3-sulfate is inferred compared with the control ligands with which DHQase binds (Fig. 5a). Following quercetin 3-sulfate, avicularin interacted with the amino acid residues of DHQase using 26 contact during simulation. Although these interactions generally occur at the same sites as those of quercetin 3-sulfate with DHQase, a transient destabilization is observed between residues 110–115 in the complex with avicularin (Fig. 5b). Galangin, in contrast, maintained only 20 contact with the DHQase residues, indicating a noticeable reduction in the binding regions the protein. Furthermore, the RMSF profile of galangin reflected higher mobility and reduced engagement with DHQase (Fig. 5c). This discrepancy in contribution ratios of RMFS plots among the three compared ligands has added an additional layer of confirmation to the identified data from the RMSD plots. This can be shown in the potential of RMSF plots to show a direct correlation between the number of ligand-protein contacts and protein stability. While quercetin 3-sulfate followed by avicularin exhibit a respectively higher number of ligand contacts in regions with lower RMSF values, more stable engagement

is suggested for these ligands, respectively. In contrast, the lower number of contacts and the higher RMSF values observed for galangin indicate greater mobility and reduced stability of its interaction with DHQase.

4. Discussion

Accumulating evidence underscores the distinctive nature of DHQase within *H. pylori*, accentuating its pivotal function as a catalyst in orchestrating the utilization of specific carbohydrates for the biosynthesis of indispensable aromatic amino acids crucial for the survival of the bacterium.⁵ This particular biochemical pathway, known

as the shikimate or chorismic pathway, is fortunately absent in mammals. What adds significance to this enzyme in our study is its potential to be targeted due to the availability of its crystallized structure (PDB ID 4B6R). Within the shikimate pathway, DHQase orchestrates the transdehydration process, facilitating the transformation of 3-dehydroquinate into 3-dehydroshikimate-a pivotal juncture in the biosynthetic route leading to the formation of aromatic amino acids.²⁸ DHQase accomplishes this task by involving three key amino acids: a proton acceptor (Tyr22), a proton donor (His102), and a transition state stabilizer (Arg17). Given this information, inhibiting any of these residues is essential to prevent the synthesis of aromatic amino acids using a library of medicinal plants from the Middle East. Notably, the positioning of Tyr22 within the active site pocket presents an intriguing opportunity for targeting DHQase, ensuring a more specific interaction of screened natural compounds within this groove. As a result, we prepared and docked the optimized chemical compounds from the Middle East library to the target groove to explore their potential to inhibit DHQase activity. In this context, it is noteworthy that quercetin 3-sulfate emerged as the ligand with the most elevated Glide docking score when assessed against the designated DHQase receptor. The collective results from molecular docking scores, Prime-MMGBSA analysis, drug-likeness assessments, toxicity predictions, and MD simulations unequivocally establish quercetin 3-sulfate as the most potent compound and a promising lead candidate. This investigation accentuates the pivotal function of quercetin 3-sulfate in the inhibition of DHQase, manifested through its establishment of a myriad of effective bonding with the residues within the active site, as evidenced by the attainment of the highest recorded docking score. Consequently, quercetin 3-sulfate can significantly reduce the biological activity of DHQase, primarily due to the comprehensive engagement of Tyr22, which forms both hydrogen bonds and Pi-Pi stacking interactions with quercetin 3-sulfate. Quercetin 3-sulfate's distinct advantage over other candidates lies in its demonstrated drug-likeness properties, as validated by ADMET assays. MD simulations were conducted for the docked quercetin 3-sulfate with DHQase alongside other candidates throughout the simulation period. The RMSD plot indicates minimal arbitrary fluctuation, signifying a more stabilized profile for the generated quercetin 3-sulfate-DHQase complex compared to other complexes. By combining the RMSF analysis with post-simulation interaction profiling, we observed that quercetin 3-sulfate engages a greater number of amino acid residues in interactions that correspond to regions of reduced flexibility. This more dynamic and stable contributions have been found to results in a more compact binding mode than that found in the other hits. Additionally, the high Prime-MMGBSA score underscores the robust binding affinity between quercetin 3-sulfate and DHQase. Unlike larger molecular weight compounds, quercetin 3-sulfate's smaller molecular weight (382.3 g/mol) is a critical factor that enables it to effectively fit inside the pocket of H. pylori DHQase with high thermodynamic efficiency. In the course of this investigation, quercetin 3-sulfate was derived from dill (Anethum graveolens), an annual herb belonging to the celery family Apiaceae, abundantly distributed across diverse Asian locales. The leaves and seeds of this botanical specimen find application both as a culinary herb, imparting flavor to various dishes, and as a nutritional supplement. However, quercetin 3-sulfate is not exclusive to dill, as quercetin, in its sulfate-free form, has been identified in many vegetables, fruits, and some spices in varying concentrations.²⁹ Quercetin, belonging to the flavonoid class of naturally occurring phytochemical agents, is known for its potent antioxidative properties, surpassing other wellknown antioxidants like vitamin C, vitamin E, and ebselen.30,31 Research endeavors have explored the potential therapeutic applications of quercetin 3-sulfate, particularly in the context of diabetes treatment. This scrutiny is based on reported observations of its capacity to enhance glucose uptake, an effect attributed to its influence on both insulin receptor signaling and glucose transport mechanisms.³² Furthermore, its potential to provide protection against oxidative stress is being explored in the context of treating Alzheimer's disease, as evidenced by pertinent publications.³³ Research has demonstrated quercetin's potential as a natural compound to effectively reduce inflammation and rheumatoid arthritis without causing adverse effects on other organs.34,35 Recent studies have revealed its anticancer properties against various cancer cell lines, suggesting quercetin's promising role in preventing, inhibiting, or even reversing carcinogenesis. Quercetin is also considered to exert a chemopreventive activity to inhibit, prevent, or even reverse carcinogenesis. 36 Notably, quercetin has shown beneficial effects against cervical, ovarian, and breast cancers, 37-39 making it a potential candidate for anticancer drug development. Quercetin, along with other flavone ring-containing compounds, exhibits a significant impact on inflammation and immune response. 40,41 Functioning as an exceptionally potent antioxidant, it stands out as a formidable scavenger of reactive oxygen-nitrogen species, thereby engendering a spectrum of diverse health benefits.³¹ Interestingly, a promising inhibitory effect against peptic ulcers in vivo has been observed when quercetin is combined with famotidine. This combination aimed to improve quercetin's intrinsic low solubility, which may have rendered it unstable in the stomach and intestinal environment due to the absence of a sulfate group. Conversely, several studies have shown that quercetin-3'-O-sulfate can be distributed in the body, exerting favorable effects in target tissues compared to quercetin alone. 42 The presence of a conjugated sulfate group introduces greater hydrophilicity into quercetin's relatively hydrophobic structure, enhancing its in vivo health benefits. 43 Despite various pharmacokinetic limitations associated with quercetin, the presence of a conjugated 3-sulfate group has addressed most of these limitations, expanding the potential applications of this compound as a potent therapeutic drug. Importantly, both quercetin and its derivative 3-sulfate conjugate comply with the Lipinski rules of druglikeness.

In terms of therapeutic potential, quercetin 3-sulfate is strongly recommended over quercetin due to the sulfate group's crucial involvement in forming hydrogen bonds with the Tyr22 residue. Conversely, quercetin, lacking the sulfate group, may significantly lose its ability to inhibit DHQase since it cannot establish direct hydrogen bonds with the Tyr22 residue. Despite various mechanisms proposed for the therapeutic effects of quercetin 3-sulfate, none have elucidated how this compound acts against H. pylori. This study provides an explanation for the mode of action in inhibiting DHQase, thereby suggesting quercetin 3-sulfate's potent therapeutic potential against these harmful pathogens. The disclosure of this information could lead to a number of in vitro and in vivo studies that are intended to confirm and validate the effectiveness of the in silico method. These endeavors, in turn, may serve to elucidate and showcase the clinical applications of this innovative methodology within the domain of antiulcer therapy. However, despite the promising findings that are obtained from this study, it is important to acknowledge the limitations of the computational approaches employed. Molecular docking and MD simulations are dependent on the accuracy of the available crystal structure and the applied force fields, which may affect the precision of the predicted binding affinities and stability. Furthermore, in silico methods do not fully replicate the complex biological environment of a living system, because multiple key factors such as metabolism, bioavailability, and off-target interactions exhibited a crucial role in determining the true therapeutic potential of the evaluated compounds. Therefore, various experimental validation through in vitro and in vivo assays will be essential to confirm the inhibitory activity and therapeutic potential of quercetin 3-sulfate against H. pylori.

5. Conclusions

Upon interacting with the designated DHQase site, quercetin 3-sulfate demonstrated the highest docking score among the medicinal plants currently investigated in the Middle East, according to the results of the virtual screening. This molecule exhibited exceptional stability and the most effective interactions with the DHQase active site residues. Importantly, quercetin 3-sulfate adhered to Lipinski's rules of druglikeness, making it a promising candidate. MD further revealed that the quercetin 3-sulfate-DHQase complex displayed more stable RMSD and RMSF plots than the other candidates. The favorable druglike properties of non-toxic quercetin 3-sulfate stood out among other natural candidates. As a result, quercetin

3-sulfate holds the potential to act as a novel inhibitor against DHQase's biological functions. This stated therapeutic potential merits further wet-lab validations to battle *H. pylori* infection and its harmful consequences on human health in the future.

Conflicts of interest

None of the authors have any financial or personal relationships that could inappropriately influence or bias the content of the paper.

Acknowledgments

The authors are grateful to Gamma Tech company (Babil, 51005, Iraq) laboratories for performing the supercomputing virtual experiments of this work. This work has been supported by Al-Qasim Green University (QGU2024-886).

6. References

- S. R. Sarhan, H. O. Hashim, M. B. S. Al-Shuhaib, Open Vet. J. 2019, 9, 339–348. DOI:10.4314/ovj.v9i4.12
- R. Vivas, A. A. T. Barbosa, S. S. Dolabela, S. Jain, *Microb. Drug Resist.* 2019, 25, 890–908. DOI:10.1089/mdr.2018.0319
- 3. S. Y. Kim, D. J. Choi, J.-W. Chung, World *J. Gastrointest. Pharmacol. Ther.* **2015**, *6*, 183. **DOI**:10.4292/wjgpt.v6.i4.183
- S. Ansari, Y. Yamaoka, Helicobacter 2017, 22, e12386.
 DOI:10.1111/hel.12386
- K. A. Ibrahim, O. M. Helmy, M. T. Kashef, T. R. Elkhamissy, M. A. Ramadan, *Pathogens* 2020, 9, 747.
 DOI:10.3390/pathogens9090747
- J. E. Kwak, J. Y. Lee, B. W. Han, J. Moon, S. H. Sohn, S. W. Suh, *Acta Crystallogr. D Biol. Crystallogr.* 2001, 57, 279–280.
 DOI:10.1107/S0907444900016267
- D. A. Robinson, K. A. Stewart, N. C. Price, P. A. Chalk, J. R. Coggins, A. J. Lapthorn, *J. Med. Chem.* 2006, 49, 1282–1290. DOI:10.1021/jm0505361
- C. L. Schmidt, H.-J. Danneel, G. Schultz, B. B. Buchanan, Plant Physiol. 1990, 93, 758–766. DOI:10.1104/pp.93.2.758
- J. Wu, J. Lv, L. Zhao, et al., Sci. Total Environ. 2023, 905, 167028. DOI:10.1016/j.scitotenv.2023.167028
- K. Saravanakumar, R. Chellia, X. Hu, K. Kathiresan, D.-H. Oh, M.-H. Wang, *Microb. Pathog.* 2019, *128*, 236–244.
 DOI:10.1016/j.micpath.2019.01.001
- M. B. S. Al-Shuhaib, S. Alam, S. A. Khan, H. O. Hashim, D. H. Obayes, J. M. B. Al-Shuhaib, *J. Biomol. Struct. Dyn.* 2023, 42, 10044–10056. DOI:10.1080/07391102.2023.2254842
- M. B. S. Al-Shuhaib, H. O. Hashim, J. M. B. Al-Shuhaib, D. H. Obayes, *J. Biomol. Struct. Dyn.* 2022, 41, 2355–2367.
 DOI:10.1080/07391102.2022.2030801
- H. O. Hashim, J. M. B. Al-Shuhaib, M. K. Mohammed, M. B. S. Al-Shuhaib, *Mol. Biotechnol.* 2024, 1–23.
 DOI:10.1007/s12033-024-01246-y

- M. B. S. Al-Shuhaib, H. O. Hashim, J. M. B. Al-Shuhaib, *Biochem. Genet.* 2024, 63, 239–60.
 DOI:10.1007/s10528-024-10709-5
- S. Kim, J. Chen, T. Cheng et al., Nucleic Acids Res. 2021, 49, D1388–D1395. DOI:10.1093/nar/gkaa971
- E. Lence, L. Tizón, J. M. Otero et al., ACS Chem. Biol. 2013, 8, 568–577. DOI:10.1021/cb300493s
- 17. V. F. Prazeres, L. Tizon, J. M. Otero *et al.*, *J. Med. Chem.* **2010**, 53,191–200. **DOI:**10.1021/jm9010466
- S. Genheden, U. Ryde, Expert Opin. Drug Discov. 2015, 10, 449–461. DOI:10.1517/17460441.2015.1032936
- R. Malikanti, R. Vadija, H. Veeravarapu, K. K. Mustyala, V. Malkhed, U. Vuruputuri, J. Mol. Struct. 2017, 1150, 227–241.
 DOI:10.1016/j.molstruc.2017.08.090
- 20. L. Dong, X. Qu, Y. Zhao, B. Wang, ACS Omega 2021, 6, 32938–32947. DOI:10.1021/acsomega.1c04996
- A. Daina, O. Michielin, V. Zoete, Sci. Rep. 2017, 7, 42717.
 DOI:10.1038/srep42717
- P. Banerjee, A. O. Eckert, A. K. Schrey, R. Preissner, *Nucleic Acids Res.* 2018, 46, W257–W263. DOI:10.1093/nar/gky318
- B. Xiao, J. Xiao, S. Liu et al., Dalton Trans. 2024, 53, 17036– 17049. DOI:10.1039/D4DT02214A
- E. Krieger, G. Vriend, J. Comput. Chem. 2015, 36, 996–1007.
 DOI:10.1002/jcc.23899
- G. Bussi, D. Donadio, M. Parrinello, J. Chem. Phys. 2007, 126, 014101. DOI:10.1063/1.2408420
- M. C. Noe, M.-C. Peakman, Drug Discovery Technologies: Current and Future Trends, 2017, 3, 1–32.
 DOI:10.1016/B978-0-12-409547-2.12312-1
- Y. Javadzadeh, S. Hamedeyaz, In: Trends in Helicobacter pylori Infection. (Ed. B. M. Roasler), IntechOpen, London, UK.
 2014, 1, 181–206. DOI:10.5772/57053
- C. Sánchez-Sixto, V. F. V. Prazeres, L. Castedo, H. Lamb, A. R. Hawkins, C. González-Bello, *J. Med. Chem.* 2005, 48, 4871–4881. DOI:10.1021/jm0501836
- 29. F. Katske, D. A. Shoskes, M. Sender, R. Poliakin, K. Gagliano,

- J. Rajfer, Tech. Urol. 2001, 7, 44-46. PMID:11272677
- A. Sokół-Łętowska, J. Oszmiański, A. Wojdyło, Food Chem.
 2007, 103, 853–859. DOI:10.1016/j.foodchem.2006.09.036
- 31. A. W. Boots, G. R. M. M. Haenen, A. Bast, *Eur. J. Pharmacol.* **2008**, 585, 325–337. **DOI**:10.1016/j.ejphar.2008.03.008
- R. Dhanya, A. D. Arya, P. Nisha, P. Jayamurthy, Front. Pharmacol. 2017, 8, 336. DOI:10.3389/fphar.2017.00336
- M. A. Ansari, H. M. Abdul, G. Joshi, W. O. Opii, D. A. Butterfield, *J. Nutr. Biochem.* 2009, 20, 269–275.
 DOI:10.1016/j.inutbio.2008.03.002
- S. M. Borghi, S. S. Mizokami, F. A. Pinho-Ribeiro *et al.*, *J. Nutr. Biochem.* 2018, 53, 81–95.
 DOI:10.1016/j.jnutbio.2017.10.010
- 35. N. Haleagrahara, S. Miranda-Hernandez, M. A. Alim, L. Hayes, G. Bird, N. Ketheesan, *Biomed. Pharmacother.* **2017**, 90, 38–46. **DOI:**10.1016/j.biopha.2017.03.026
- A. Murakami, H. Ashida, J. Terao, Cancer Lett. 2008, 269, 315–325. DOI:10.1016/j.canlet.2008.03.046
- R. V. Priyadarsini, R. S. Murugan, S. Maitreyi, K. Ramalingam, D. Karunagaran, S. Nagini, *Eur. J. Pharmacol.* 2010, 649, 84–91. DOI:10.1016/j.ejphar.2010.09.020
- R. Shafabakhsh, Z. Asemi, J. Ovarian Res. 2019, 12, 1–9.
 DOI:10.1186/s13048-019-0530-4
- R. L. Singhal, Y. A. Yeh, N. Prajda, E. Olah, G. W. Sledge, G. Weber, *Biochem. Biophys. Res. Commun.* 1995, 208, 425–431.
 DOI:10.1006/bbrc.1995.1355
- S. Chirumbolo, *Inflamm. Allergy Drug Targets* 2010, 9, 263–285. DOI:10.2174/187152810793358741
- G. Carullo, A. R. Cappello, L. Frattaruolo, M. Badolato, B. Armentano, F. Aiello, *Future Med. Chem.* 2017, 9, 79–93.
 DOI:10.4155/fmc-2016-0186
- 42. K. Kawabata, R. Mukai, A. Ishisaka, Food Funct. **2015**, 6, 1399–1417. **DOI**:10.1039/C4FO01178C
- 43. Y. Kawai, *J. Med. Investig.* **2018**, 65, 162–165. **DOI:**10.2152/jmi.65.162

Povzetek

Dehidrokinaza tipa II (DHQase) je ključni encim pri sintezi aromatskih aminokislin, ki so nujne za preživetje bakterije *Helicobacter pylori*. Kaže posebne lastnosti in ima le malo sekvenčne ali strukturne podobnosti z encimi v drugih bakterijah. Za presejanje spojin, ki jih najdemo v zdravilnih rastlinah s Srednjega vzhoda, smo uporabili molekularno sidranje da bi našli najbolj obetavne spojine za zaviranje DHQase z največjo afiniteto. Sidrali smo 2.213 konformerjev ligandov, pridobljenih iz 151 zdravilnih rastlin. Izmed njih smo izbrali deset spojin z najboljšimi rezultati sidranja za nadaljnjo analizo ADMET in simulacijo molekulske dinamike. Med najboljšimi kandidati je najvišjo oceno sidranja deosegel kvercetin-3-sulfat. Spojina izpolnjuje kriterije primernosti za zdravilo in ne kaže toksicnosti. Simulacije molekulske dinamike so pokazale, da kompleks med kvercetin-3-sulfatom in DHQase dosega bolj stabilen RMSD profil in večjo stabilizacijo s strani sosednjih aminokislinskih ostankov kot druge spojine iz te študije. Raziskava izpostavi kvercetin-3-sulfat kot obetavno spojino za zaviranje DHQase, saj kaže najvišjo afiniteto liganda. Rezultati nakazujejo, da je kvercetin-3-sulfat obetaven kandidat za zdravljenje okužb s *H. pylori*.



Except when otherwise noted, articles in this journal are published under the terms and conditions of the Creative Commons Attribution 4.0 International License